

**BOUNDARY-LAYER, PRESSURE, AND TEMPERATURE  
DISTRIBUTION STUDIES ON SEVERAL ISENTROPIC  
COMPRESSION SURFACES AT MACH NUMBERS  
FROM 4 TO 8**

This document has been approved for public release  
its distribution is unlimited.

By

R. W. Rhudy and F. K. Hube  
von Kármán Gas Dynamics Facility  
ARO, Inc.

*Per DDC TR-75/5  
AD A011700  
D+I July 1975*

**TECHNICAL DOCUMENTARY REPORT NO. AEDC-TDR-64-268**

**December 1964**

**Program Element 62405334/ Project 1366, Task 136605**

(Prepared under Contract No. AF 40(600)-1000 by ARO, Inc.,  
contract operator of AEDC, Arnold Air Force Station, Tenn.)

**ARNOLD ENGINEERING DEVELOPMENT CENTER  
AIR FORCE SYSTEMS COMMAND  
UNITED STATES AIR FORCE**

AEDC TECHNICAL LIBRARY

5 0720 00040 0699

PROPERTY OF U. S. AIR FORCE  
AEDC LIBRARY  
AF 40(600)1000

# ***NOTICES***

Qualified requesters may obtain copies of this report from DDC, Cameron Station, Alexandria, Va. Orders will be expedited if placed through the librarian or other staff member designated to request and receive documents from DDC.

When Government drawings, specifications or other data are used for any purpose other than in connection with a definitely related Government procurement operation, the United States Government thereby incurs no responsibility nor any obligation whatsoever; and the fact that the Government may have formulated, furnished, or in any way supplied the said drawings, specifications, or other data, is not to be regarded by implication or otherwise as in any manner licensing the holder or any other person or corporation, or conveying any rights or permission to manufacture, use, or sell any patented invention that may in any way be related thereto.

BOUNDARY-LAYER, PRESSURE, AND TEMPERATURE  
DISTRIBUTION STUDIES ON SEVERAL ISENTROPIC  
COMPRESSION SURFACES AT MACH NUMBERS  
FROM 4 TO 8

By

R. W. Rhudy and F. K. Hube  
von Kármán Gas Dynamics Facility

ARO, Inc.

a subsidiary of Sverdrup and Parcel, Inc.

December 1964

ARO Project No. VT0306

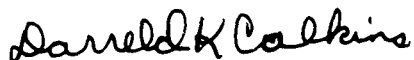
References to named commercial products in this report are not to be considered in any sense as an endorsement of the product by the United States Air Force or the Government.

**ABSTRACT**


Boundary-layer, pressure, and temperature measurements were obtained on the generating cylinder and isentropic compression surface of several axisymmetric hypersonic inlet configurations at supersonic and hypersonic Mach numbers. Boundary-layer surveys were performed at selected stations on uncooled Mach 5, 6, and 10 inlets and a cooled Mach 8 inlet. Model surface temperatures and pressures were obtained at several Mach numbers on all configurations. Steady-state heat transfer data were obtained on the Mach 8 inlet at several model wall temperatures. Selected results from the tests are presented.

**PUBLICATION REVIEW**

This report has been reviewed and publication is approved.



Darreld K. Calkins  
Major, USAF  
AF Representative, VKF  
DCS/Test



Jean A. Jack  
Colonel, USAF  
DCS/Test

## CONTENTS

	<u>Page</u>
ABSTRACT . . . . .	iii
NOMENCLATURE . . . . .	vii
1.0 INTRODUCTION . . . . .	1
2.0 APPARATUS	
2.1 Wind Tunnels . . . . .	1
2.2 Models . . . . .	2
2.3 Cooling System . . . . .	3
2.4 Boundary-Layer Surveying Equipment . . . . .	3
2.5 Boundary-Layer Probes . . . . .	3
2.6 Instrumentation . . . . .	4
3.0 PROCEDURE	
3.1 Test Procedure . . . . .	5
3.2 Data Reduction Procedure . . . . .	6
4.0 RESULTS AND DISCUSSION . . . . .	7

## TABLES

1. Model Compression Surface Coordinates . . . . .	9
2. Test Run Summary . . . . .	11

## ILLUSTRATIONS

Figure

1. Tunnel A . . . . .	13
2. Tunnel B . . . . .	14
3. General Model Dimensions . . . . .	15
4. Inlet and Trip Geometry for the Mach 5, 6, and 10 Models . . . . .	16
5. Inlet and Trip Geometry for the Mach 8 Model . . . . .	17
6. Mach 8 Model Cooling Passages . . . . .	18
7. Typical Model Installation in Tunnel A	
a. C <sup>10</sup> G <sup>17</sup> TVGF . . . . .	19
b. C <sup>8</sup> G <sup>12.5</sup> TVGF . . . . .	20

<u>Figure</u>	<u>Page</u>
8. Typical Model Installation in Tunnel B	
a. General Sketch . . . . .	21
b. C <sup>5</sup> G <sup>9</sup> T VGF . . . . .	22
c. C <sup>8</sup> G <sup>12.4</sup> T VGF . . . . .	23
9. Cooling System for Mach 8 Model . . . . .	24
10. Geometry of the Triple Survey Probe . . . . .	25
11. Triple Survey Probe Installed in Tunnel B . . . . .	26
12. Typical Thermocouple Plug Wiring Diagram . . . . .	27
13. Compression Surface Pressure Distribution at Various Mach Numbers	
a. C <sup>5</sup> G <sup>17</sup> T VGF . . . . .	28
b. C <sup>6</sup> G <sup>17</sup> T VGF . . . . .	29
c. Mach 8 Model . . . . .	30
d. C <sup>10</sup> G <sup>17</sup> T VGF . . . . .	31
14. Boundary-Layer Thickness for All Models at M <sub>∞</sub> = 6, Re/ft = 4.6 x 10 <sup>6</sup> . . . . .	32
15. Velocity Profiles for All Models at or near Design Mach Number. . . . .	33
16. Effect of Model Wall Temperature on Velocity Profile	
a. x/ℓ = 0 . . . . .	34
b. x/ℓ = 0.96 . . . . .	34
17. Effect of Model Wall Temperature on Boundary-Layer Thickness . . . . .	35

## NOMENCLATURE

$b$	Thermocouple plug thickness, ft
$h$	Heat transfer coefficient, Btu/hr ft <sup>2</sup> °R
$K$	Thermal conductivity of model material, Btu-ft/hr ft <sup>2</sup> °R
$l$	Reference length, (from start of compression surface to last instrumented station), in.
$M_{\infty}$	Free-stream Mach number
$p$	Local static pressure, psia
$p_O$	Tunnel stagnation pressure, psia
$p_w$	Model surface pressure, psia
$p_{\infty}$	Free-stream static pressure, psia
$\dot{q}$	Heat flux, Btu/hr ft <sup>2</sup>
$Re_{\infty}$	Free-stream unit Reynolds number, per ft
$T_{AW}$	Adiabatic wall temperature, °R
$T_{Diff}$	Differential temperature measured from model, °R (Note 4, Fig. 12)
$T_I$	Model internal temperature, °R
$T_O$	Tunnel stagnation temperature, °R
$T_S$	Model surface temperature, °R
$U$	Local velocity, ft/sec
$U_{\infty}$	Free-stream velocity, ft/sec
$x$	Model axial station (positive values are on the compression surface and negative values are on the generating cylinder, Fig. 3), in.
$Y$	Distance in the boundary layer normal to model surface, in.
$Z$	Model radius normal to the $x$ axis, in.
$\delta$	Boundary-layer thickness, in.

## MODEL NOMENCLATURE

$C^5$	Mach 5 compression surface
$C^6$	Mach 6 compression surface



C <sup>8</sup>	Mach 8 compression surface
C <sup>10</sup>	Mach 10 compression surface
G <sup>9</sup>	9-in. generating cylinder
G <sup>12.4</sup>	12.4-in. generating cylinder
G <sup>17</sup>	17-in. generating cylinder
G <sup>25</sup>	25-in. generating cylinder
T <sup>VGf</sup>	Vortex generator trip (forward position)
T <sup>VGR</sup>	Vortex generator trip (aft position)
T <sup>VGfR</sup>	T <sup>VGf</sup> + T <sup>VGR</sup>

## 1.0 INTRODUCTION

At the request of the Aeronautical Systems Division, Air Force Systems Command (ASD-AFSC), boundary-layer survey, pressure distribution, and heat transfer tests were conducted on several hypersonic compression surfaces for the Lockheed-California Company at nominal Mach numbers of 4, 5, 6, and 8 and free-stream Reynolds numbers from  $0.5 \times 10^6$  to  $6.6 \times 10^6$  per foot. The tests were performed in the 40-in. supersonic tunnel (Gas Dynamic Wind Tunnel, Supersonic (A)) and the 50-in. Mach 8 tunnel (Gas Dynamic Wind Tunnel, Hypersonic (B)) of the von Kármán Facility (VKF), Arnold Engineering Development Center (AEDC), AFSC, at intermittent periods from March 20, 1963 to September 28, 1964.

Boundary-layer surveys were made at selected stations along the models with emphasis on the aft stations in the region of the adverse pressure gradients. The Mach 5 and 6 inlets were tested at Mach numbers of 4, 5, and 6; the Mach 8 inlet was tested at Mach numbers of 5, 6, and 8; and the Mach 10 inlet was tested at Mach numbers of 4, 5, 6, and 8. Model surface pressures and temperatures were also recorded. All data were taken with the models at zero angle of attack.

## 2.0 APPARATUS

### 2.1 WIND TUNNELS

#### 2.1.1 Tunnel A

Tunnel A is a 40- by 40-in. supersonic, continuous, closed circuit, variable density wind tunnel with an automatically driven flexible plate-type nozzle (Fig. 1). The tunnel operates at Mach numbers from 1.5 to 6 at maximum stagnation pressures from 29 to 200 psia, respectively, and stagnation temperatures up to 300°F ( $M_\infty = 6$ ). Minimum operating pressures are about one-tenth of the maximum at each Mach number.

#### 2.1.2 Tunnel B

Tunnel B is a Mach 8, axisymmetric, continuous flow, variable density, wind tunnel with a 50-in. -diam test section (Fig. 2). Because

---

Manuscript received November 1964.

of changes in boundary-layer thickness caused by changing pressure level, the Mach 8 contoured nozzle produces an average test section Mach number which varies from 8.0 at a stagnation pressure of 100 psia to 8.1 at 800 psia. The maximum stagnation temperature of 900°F is sufficient to prevent liquefaction of air in the test section. There is a slight axial gradient on the order of 0.01 Mach number per foot. A more complete description of the tunnels and associated equipment is given in the Test Facilities Handbook\*.

## 2.2 MODELS

All models consisted of an inlet to which a boundary-layer trip was attached, a generating cylinder, and an isentropic compression surface. The type of boundary-layer trip and length of the generating cylinder were varied during the test in an attempt to determine the best combination to obtain turbulent boundary layer ahead of the compression surface. The general geometry of all models is shown in Fig. 3, and the details of the trips are shown in Figs. 4 and 5. The coordinates for the various model compression surfaces are presented in Table 1.

All models were instrumented with surface pressure orifices and thermocouples. The Mach 8 model was also instrumented with nine pairs of thermocouples to obtain steady-state heat transfer data. Each pair of thermocouples was installed in a plug with one couple located on the internal surface and the other on the external surface. The hookup of the thermocouples is described in detail later. This model also contained internal passages for cooling (Fig. 6) which permitted data to be obtained at several model surface temperatures. The final model surface temperatures were fairly uniform except on the aft portion of the compression surface at Mach 8 where the temperatures varied from 50 to 100°F higher than the rest of the model because of model construction.

As shown in Fig. 7, the models were mounted on the main model support system by means of an offset adaptor. The adapter for the Mach 8 configuration was somewhat different than that for the other models because the model was larger, and coolant passages were required. In Tunnel B all of the models were mounted from the tunnel side wall as shown in Fig. 8.

---

\*Test Facilities Handbook, (5th Edition). von Kármán Gas Dynamics Facility, Vol. 4. Arnold Engineering Development Center, July 1963.

## 2.3 COOLING SYSTEM

The cooling system for the internally cooled Mach 8 model consisted of a high pressure air supply, part of which was passed through a heat exchanger. The coolant used in the heat exchanger was liquid nitrogen. With this system (Fig. 9) air temperatures sufficient to cool the model surface to approximately  $-40^{\circ}\text{F}$  were obtained except on the aft compression surface at Mach 8, as previously stated.

## 2.4 BOUNDARY-LAYER SURVEYING EQUIPMENT

The boundary-layer probe drive mechanism is capable of translating the probe 4.3 in. in a direction parallel to the probe arm. The probe arm can also be pitched through an angle of  $35^{\circ}$ . Two low speed d-c motors were used to drive the mechanism. The probe head, which contained motors, transducers, and potentiometers, was protected from the tunnel temperature by a water jacket. Other water lines and passages were routed throughout the system to ensure adequate cooling of the mechanism.

The boundary-layer probe head was mounted on the shaft of a 50-in. surveying unit which provides 50 in. of longitudinal movement. In Tunnel B the shaft traversed through the roll mechanism and sector and attached to a hydraulic servo unit mounted downstream from the sector. In Tunnel A the hydraulic unit was also downstream from the sector, but the shaft centerline was 8.25 in. above the tunnel centerline.

## 2.5 BOUNDARY-LAYER PROBES

Measurements in the boundary layer were made with a triple probe consisting of a total pressure, static pressure, and total temperature probes. The geometry of the probe tip is shown in Figs. 10 and 11. The pitot (total pressure) probe was fabricated of stainless steel tubing which stepped down from 0.125 in. OD (0.095-in. ID) tubing to 0.020-in. OD (0.10-in. ID) tubing in several increments. A 0.063-in. OD piece of tubing was insulated with Fiberglas tape and mounted inside the 0.125-in. OD tubing electrically isolating the tip of the pitot probe from the probe support. A grounding light connected to this tube indicated when the pitot tube was in contact with the model surface. The static pressure probe was 0.030-in. in diameter and had four 0.006-in. -diam orifices placed at  $45^{\circ}$  to the vertical and horizontal planes of the probe. The total temperature probe consisted of a chromel-alumel thermocouple placed inside a 0.040-in. -diam single radiation shield.

## 2.6 INSTRUMENTATION

### 2.6.1 Tunnel Pressure System

Model pressures in Tunnel A were measured with nine pairs (a 1 psid and a 15 psid) of Wiancko transducers referenced to vacuum. The 1-psid transducers were calibrated to obtain full-scale deflections at 0.16, 0.40, and 1.0 psid; the 15-psid transducers were calibrated at 2.4, 6.0, and 15 psid. The system automatically selects the appropriate transducer and sensitivity for the pressure being measured. Some of the pressures in Tunnel A were also measured with CEC Electromanometers rated at 1, 5, and 15 psia.

The model pressures in Tunnel B were measured with nine Wiancko pressure transducers, rated at 5 psid, connected selectively to seven independently variable reference pressures which were constantly monitored by seven CEC Electromanometers rated at 1, 5, 15, and 30 psia.

This system will automatically select the proper instrument sensitivity and absolute reference pressure to ensure measurement of the model pressures to the best available precision. Three instrument sensitivities, calibrated to obtain full-scale deflection for  $\pm 0.3$ ,  $\pm 0.6$ , and  $\pm 1.2$  psid were used in conjunction with the seven reference pressures which varied in approximately 2-psia increments from nearly zero pressure.

For both Tunnel A and Tunnel B the pressure side of each Wiancko transducer was inserted into the outlet of a Giannini 12-position rotary valve. Reference pressure was connected to the first valve inlet position to obtain the instrument zero. Various model pressure taps were connected in the desired order to the required number of the remaining 11 valve inlets. The transducer outputs were measured with Leeds and Northrup self-balancing, millivolt potentiometers equipped with Coleman digital readout units. The potentiometer readings were recorded on paper tapes with a high-speed punch.

### 2.6.2 Model Temperatures

The model surface temperatures were measured with chromel-alumel thermocouples which were connected to an automatically stepping temperature scanner capable of handling four temperatures simultaneously. Thermocouple outputs were measured with Leeds and Northrup self-balancing, millivolt potentiometers equipped with Coleman digital readout units.

The nine pairs of thermocouples on the Mach 8 model were connected to a Beckman 210 analog-to-digital converter and data recorded for each

model wall temperature. These thermocouples were supplemented by the addition of a common stainless lead to each of the constantan leads providing another nine pairs of thermocouples as a check. The thermocouple installation and hookup are shown in Fig. 12.

### 2.6.3 Probe Instrumentation

The pitot pressures were measured with a 15-psid Wiancko transducer for one phase of the test and a 50-psid Wiancko transducer for the other. The transducers were calibrated for full-scale deflections of 0.5, 1, 2, 3, 6 and 12 psid for the 15 psid and 0.5, 1, 2, 10, 20, and 40 psid for the 50 psid. The static probe pressures were measured with a 5-psid Wiancko transducer calibrated for full-scale deflections of approximately 0.15, 0.30, 0.60, 1.2 and 2.4 psid. Both transducers were mounted in the probe head to reduce the length of the pressure leads and minimize the lag times. Instrument zeros could be taken at any time by actuating a dual, two position, air operated valve which was also mounted inside the probe head.

The chromel-alumel thermocouple from the total temperature probe was monitored with a Leeds and Northrup millivolt potentiometer.

Probe height readings ("Y" measurements) were obtained by means of a 0.1-percent ten turn potentiometer connected to the drive motor by a slip clutch and a gear train. Ten turns of the potentiometer corresponded to approximately 1 in. of travel. The 0.1-percent potentiometer output was measured with a null-balancing potentiometer equipped with a Coleman digital readout unit. The output of a 0.5-percent slide wire potentiometer, measured with a digital voltmeter, was used to determine the angle of the probe arm. The variation of the output was non-linear with angle, and the angle as obtained from a calibration curve was recorded by manual input.

## 3.0 PROCEDURE

### 3.1 TEST PROCEDURE

The tunnel was brought to operating conditions, the model was allowed to "soak" until a stable surface temperature was reached, and the model surface pressures and temperatures were recorded. The probe arm was pitched to the proper angle so that all surveys were determined normal to the model surface. The survey probe was then positioned and lowered to the model surface at the station to be surveyed. The probe was lowered until the light indicated when the pitot tube was in contact with the

model surface, and the survey was started at this point. Approximately 20 to 25 data points were taken at various increments for each survey. After the desired model stations were surveyed at a particular condition, another tunnel condition was set and the procedure repeated. The above procedure was followed for the Mach 5, 6, and 10 models. A similar procedure was followed for the Mach 8 model except the model surface was cooled to a particular temperature before the surveys were started.

### 3.2 DATA REDUCTION PROCEDURE

#### 3.2.1 Heat Transfer Data

The heat transfer data obtained from the Mach 8 model were reduced on the AEDC IBM 7074 computer using the equations listed below. The values of  $\dot{q}$  were obtained by two methods as shown in these equations. Two values of  $h$  were then obtained using the two values of  $\dot{q}$ .

$$\dot{q}_1 = \frac{K (T_{Diff})}{b} \quad (1)$$

$$\dot{q}_2 = \frac{K (T_s - T_I)}{b} \quad (2)$$

where  $K$  is a function of model surface temperature at the point on the model where  $\dot{q}$  is being evaluated, and

$$h = \frac{\dot{q}}{T_{AW} - T_s} \quad (3)$$

This procedure was followed for the nine pairs of thermocouples on the model.

#### 3.2.2 Boundary-Layer Data

Because of the curvature of the compression surface of the model and the triple probe geometry, the height above the surface ( $Y$ ) of the static pressure probe and the temperature probe was not the same as the pitot probe. This variation was compensated for by equations in the computer program and interpolation of the preliminary data. The final data reduction of the boundary-layer surveys was accomplished on the AEDC IBM 7074 computer.

The static pressure profiles were determined from the model wall pressure, the static probe measurements, and computed static pressure outside the boundary layer. The static pressures in the boundary layer on the generating cylinder were assumed to be constant. The static

pressures outside the boundary layer on the compression surface were determined from the computed total pressure behind the inlet shock and the measured local pitot pressures.

The temperature probe recovery factor was determined from a calibration using measurements in the free-stream at several Reynolds numbers. With the pitot pressure, static pressure, and total temperature determined, additional parameters of the boundary layer were calculated.

The boundary-layer thickness ( $\delta$ ) was defined as the point where the total pressure began to deviate from the total pressure outside the boundary layer. Numerical values of the boundary-layer thickness were determined graphically from pitot profiles and static pressure profiles. The computed static pressures assume a constant total pressure and are valid outside the boundary layer only. Computed values inside the boundary layer deviate sharply from the measured values; this point of deviation was assumed to be the boundary-layer thickness, i. e.,  $Y = \delta$ . Values of momentum thickness, displacement thickness, form factor, and local density for viscous and inviscid flow were also calculated and tabulated on the data.

#### 4.0 RESULTS AND DISCUSSION

A complete test run summary is given in Table 2 and indicates the scope of the investigation. The test program was so extensive that an attempted data analysis is impractical for this discussion, and the results presented are limited to representative plots of the basic data obtained on the four model configurations for selected test conditions.

The compression surface pressure distributions obtained on the various models at several Mach numbers are shown in Fig. 13. The data presented for the Mach 8 model in this figure are for the uncooled condition. These results show that the static pressure recovery along the isentropic compression surface increased with increasing Mach number for each configuration, but not as much as predicted by inviscid theory. Within the accuracy of the data, there is no loss of total pressure from the beginning to the end of the compression surface; however, there is a small loss across the generating cylinder and the boundary-layer trips. This loss and the presence of the boundary layer on the compression surface cause the difference between the experimental and the ideal inviscid pressure recovery values.



The boundary-layer thickness along the models at a free-stream Mach number of 6 is presented in Fig. 14. This figure indicates very little difference in the boundary-layer thickness for the Mach 5 and Mach 6 models while the boundary layer was thicker on the aft portion of the Mach 10 model and on the Mach 8 model from station 0 to an  $x/\ell$  of approximately 0.96.

Typical velocity profiles for the four models at or near design Mach number are shown in Fig. 15. The data are presented at the start of the compression surface and for the aft station surveyed. This figure shows very little variation in the profiles obtained at the two extremes of the compression surface, and the profiles indicate a turbulent boundary layer along the compression surface for each inlet configuration.

Figure 16 shows the effect of model wall temperature on the boundary-layer velocity profiles for the Mach 8 model at  $x/\ell = 0$  and 0.96. The wall temperatures listed are nominal as there were some variations in these temperatures because of the difficulties encountered with the model cooling system. These curves indicate that the model wall temperature had very little effect on the boundary-layer profiles. These slight variations were less evident on the aft portion than on the forward port of the compression surface.

The changes in boundary-layer thickness along the Mach 8 model at several surface temperatures are shown in Fig. 17. Although there were difficulties in maintaining each wall temperature while the boundary-layer surveys were obtained at the various model stations, the results in general show the model wall temperature to have little effect on the boundary-layer thickness on the cylindrical and compression surfaces of the model for the wall temperatures investigated.

**TABLE 1**  
**MODEL COMPRESSION SURFACE COORDINATES**

Mach 5 Model

<u>x</u>	<u>Z</u>	<u>x</u>	<u>Z</u>	<u>x</u>	<u>Z</u>
0.001	1.000	10.064	1.749	15.803	3.055
1.368	1.013	10.558	1.832	16.066	3.147
2.626	1.050	11.072	1.914	16.301	3.233
3.778	1.104	11.520	1.994	16.510	3.314
4.830	1.169	12.319	2.148	16.784	3.427
5.791	1.244	13.009	2.294	17.017	3.530
6.668	1.324	13.608	2.432	17.267	3.653
7.470	1.408	14.131	2.562	17.487	3.762
8.204	1.493	14.588	2.684	17.736	3.904
8.877	1.579	14.990	2.798	18.022	4.094
9.495	1.664	15.507	2.957	18.157	4.198

Mach 6 Model

0.000	1.000	14.722	2.455	17.295	3.281
2.951	1.052	15.140	2.560	17.398	3.329
5.357	1.172	15.502	2.658	17.491	3.373
7.314	1.323	15.818	2.749	17.574	3.415
8.913	1.484	16.094	2.833	17.648	3.454
10.230	1.645	16.336	2.912	17.774	3.524
11.325	1.801	16.548	2.985	17.877	3.568
12.243	1.950	16.736	3.053	17.979	3.652
13.017	2.089	16.901	3.116	18.029	3.688
13.675	2.220	17.048	3.175	18.073	3.720
14.238	2.341	17.179	3.230	18.110	3.749

TABLE 1 (Concluded)

## Mach 8 Model

<u>x</u>	<u>Z</u>	<u>x</u>	<u>Z</u>	<u>x</u>	<u>Z</u>
0.004	1.500	26.316	3.218	32.988	4.545
2.026	1.509	27.122	3.340	33.208	4.606
5.709	1.575	28.188	3.516	33.508	4.694
8.928	1.683	28.816	3.627	33.776	4.776
10.382	1.748	29.388	3.732	34.012	4.851
11.739	1.816	29.907	3.831	34.226	4.923
14.196	1.966	30.381	3.927	34.476	5.010
16.350	2.122	31.016	4.062	34.790	5.127
18.243	2.280	31.570	4.186	35.082	5.246
20.678	2.514	31.944	4.266	35.313	5.346
22.072	2.666	32.210	4.340	35.565	5.468
23.316	2.811	32.490	4.412	35.919	5.667
24.426	2.952	32.750	4.479	36.064	5.768
25.420	3.087				

## Mach 10 Model

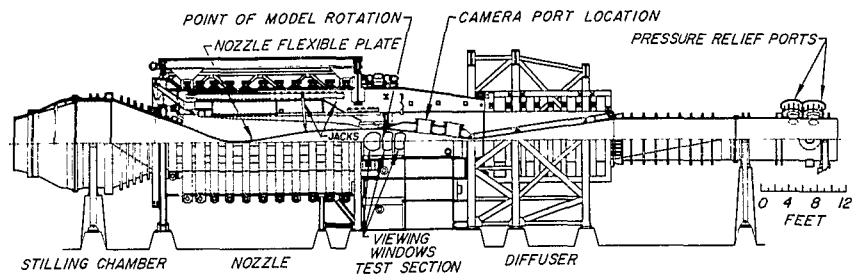
0.000	1.000	15.754	1.712	22.783	2.817
1.614	1.007	16.619	1.802	22.891	2.847
3.110	1.026	17.722	1.930	22.990	2.875
4.490	1.054	18.636	2.048	23.080	2.902
5.762	1.089	19.399	2.156	23.240	2.951
6.935	1.129	19.839	2.223	23.314	2.994
8.017	1.173	20.412	2.317	23.515	3.043
9.015	1.220	20.899	2.403	23.688	3.109
9.938	1.268	21.182	2.456	23.843	3.174
10.792	1.318	21.556	2.530	23.984	3.242
11.582	1.369	21.974	2.619	24.103	3.310
12.315	1.419	22.238	2.680	24.150	3.342
13.628	1.519	22.536	2.752		
14.765	1.617	22.725	2.802		

**TABLE 2**  
**TEST RUN SUMMARY**

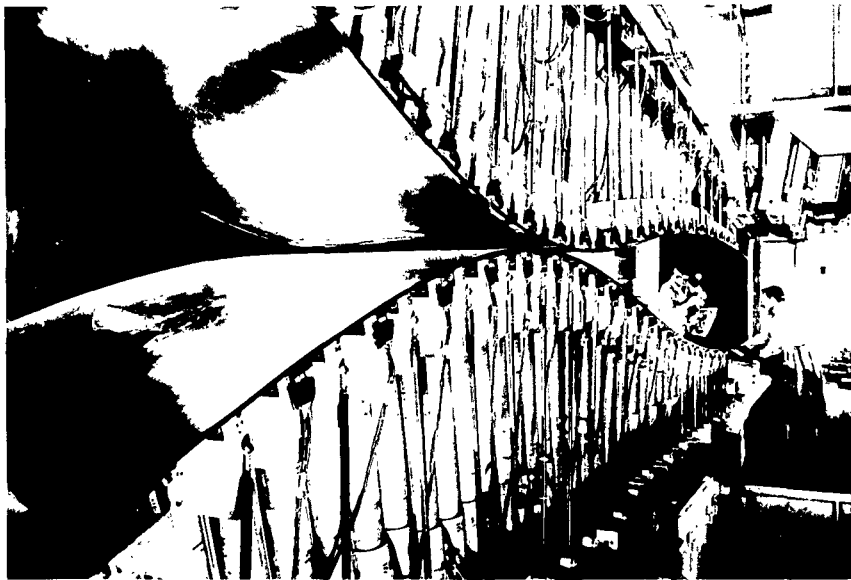
Configuration	$M_\infty$	$p_0$ , psia	$Re/ft \times 10^{-6}$	Stations Surveyed
C <sup>10</sup> G <sup>17</sup> TVGF	8	800	3.4	-9.5, -3.5, -0.5, 12.5, 20, 22, 23, 24
		500	2.2	
		300	1.6	-9.5, -3.5, -0.5
	6	200	4.6	-9.5, -3.5, -0.5, 12.5, 20, 22, 23, 24
		100	2.3	
	5	150	6.6	-0.5, 12.5, 20, 22, 23, 24
		40	1.8	
	4	75	6.0	-0.5, 12.5, 20, 22, 23, 24
		10	0.84	
C <sup>10</sup> G <sup>9</sup> TVGF	8	800	3.4	-0.5, -4.5, 12.5, 20, 22, 23, 24
		500	2.2	
C <sup>10</sup> G <sup>9</sup> TVGFR	8	800	3.4	-0.5, -4.5, 12.5, 20, 22, 23, 24
C <sup>5</sup> G <sup>17</sup> TVGF	6	200	4.6	-9.5, -3.5, -0.5, 8.5, 14, 17, 18
		100	2.3	
	5	150	6.6	-9.5, -3.5, -0.5, 8.5, 14, 17, 18
		40	1.8	
	4	75	6.0	-9.5, -3.5, -0.5, 8.5, 14, 17, 18
		10	0.84	
C <sup>5</sup> G <sup>9</sup> TVGF	6	200	4.6	-0.5, 8.5, 14, 17, 18
		100	2.3	
	5	150	6.6	-4.5, -0.5, 8.5, 14, 17, 18
		40	1.8	
	4	75	6.0	-4.5, -0.5, 8.5, 14, 17, 18
		10	0.84	
C <sup>6</sup> G <sup>17</sup> TVGF	6	200	4.6	-0.5, 8.5, 14, 17, 18
		100	2.3	

TABLE 2 (Concluded)

Configuration	$M_\infty$	$p_o$ , psia	$Re/ft \times 10^{-6}$	Wall Temp, °R	Station Surveyed
$C^8 G^{12.4} T^{VGF}$	5	150	6.6	400	-7.5, 0, 18.75, 29, 33,
		40	1.8	400	34.5, 36
	5	150	6.6	480	-7.5, 0, 18.75, 29, 33,
		40	1.8	480	34.5, 36
	5	150	6.6	Uncooled	-7.5, 0, 18.75, 29, 33,
		40	1.8		34.5, 36
	6	200	4.6	400	-7.5, 0, 18.75, 29, 33,
		100	2.3	400	34.5, 36
	6	200	4.6	506	-7.5, 0, 18.75, 29, 33,
		100	2.3	506	34.5, 36
	6	200	4.6	Uncooled	-7.5, 0, 18.75, 29, 33,
		100	2.3		34.5, 36
$C^8 G^{12.4} T^{VGFR}$	8	800	3.4	Uncooled	0, 18.75, 29, 33, 34.5
$C^8 G^{25} T^{VGF}$	8	800	3.4	490	-16.5, -7.5, 0, 18.75, 29,
		335	1.6	490	33, 34.5, 36
	8	800	3.4	590	-16.5, -7.5, 0, 18.75, 29,
		335	1.6	590	33, 34.5, 36
	8	800	3.4	850	-16.5, -7.5, 0, 18.75, 29,
		335	1.6	850	33, 34.5, 36
	8	800	3.4	Uncooled	-16.5, -7.5, 0, 18.75, 29,
					33, 34.5, 36



Assembly



Nozzle and Test Section

Fig. 1 Tunnel A

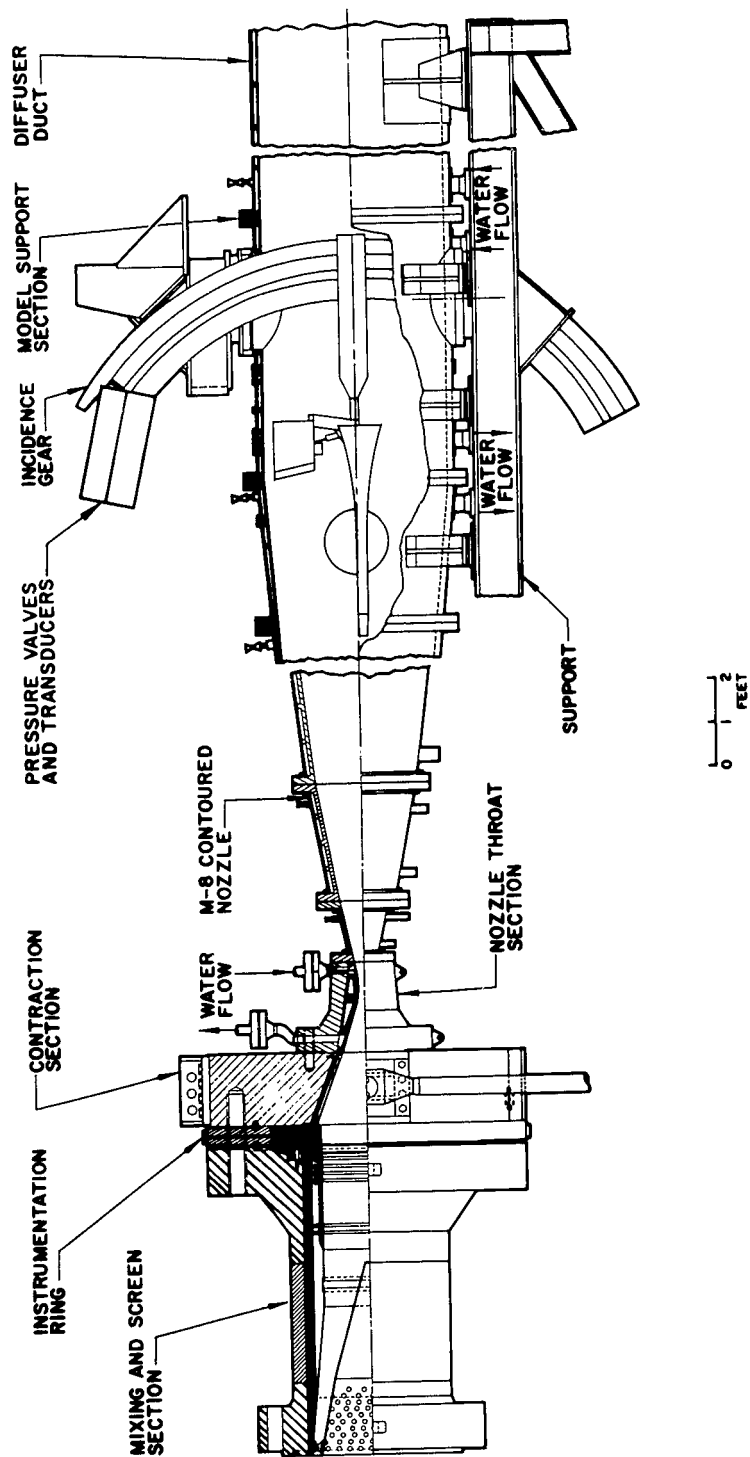
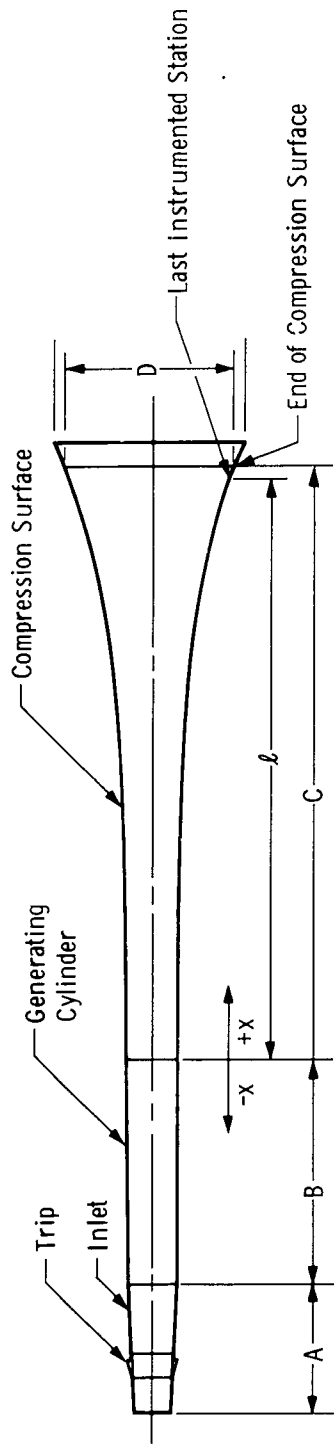


Fig. 2 Tunnel B



All Dimensions in Inches

CONFIGURATION	A	B	C	D	$\ell$
C <sup>10</sup> G <sup>17</sup> T VGF	5.286	17.0	24.15	6.684	24.00
C <sup>10</sup> G <sup>9</sup> T VGF & C <sup>10</sup> G <sup>9</sup> T VGF R	5.286	9.0	24.15	6.684	24.00
C <sup>5</sup> G <sup>17</sup> T VGF	5.286	17.0	18.157	8.396	18.15
C <sup>5</sup> G <sup>9</sup> T VGF	5.286	9.0	18.157	8.396	18.15
C <sup>6</sup> G <sup>17</sup> T VGF	5.286	17.0	18.110	7.498	18.10
C <sup>8</sup> G <sup>12.4</sup> T VGF & C <sup>8</sup> G <sup>12.4</sup> T VGF R	9.75	12.4	36.75	12.377	36.00
C <sup>8</sup> G <sup>25</sup> T VGF	9.75	25.0	36.75	12.377	36.00

Fig. 3 General Model Dimensions

104132



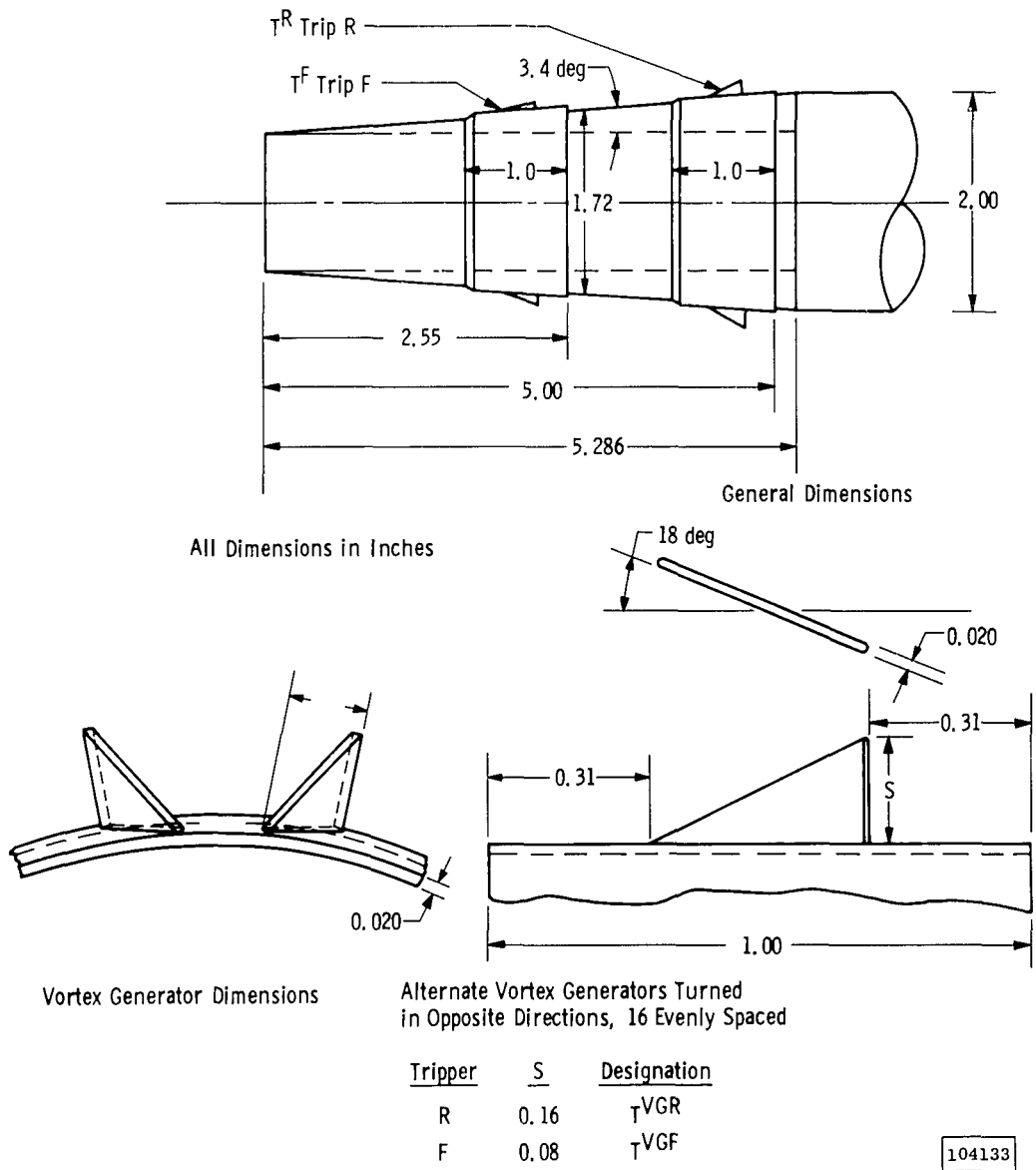


Fig. 4 Inlet and Trip Geometry for the Mach 5, 6, and 10 Models

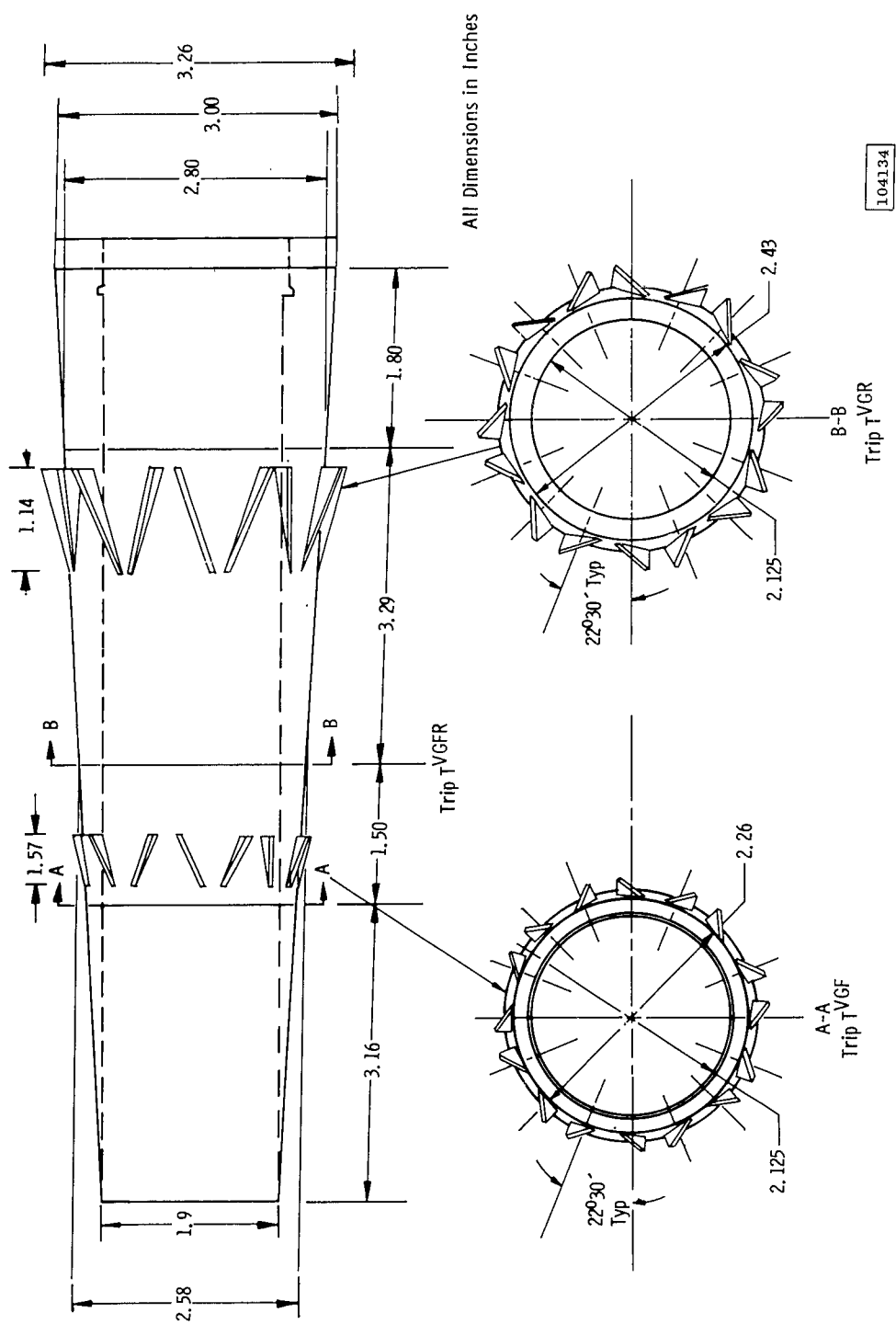


Fig. 5 Inlet and Trip Geometry for the Mach 8 Model

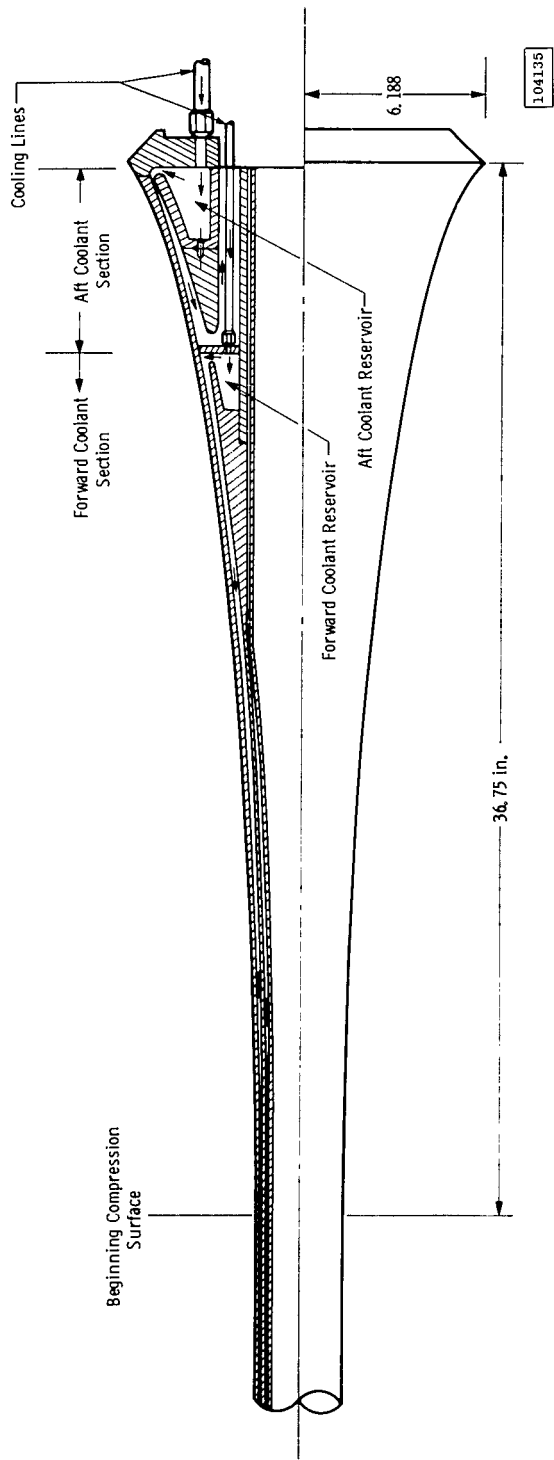
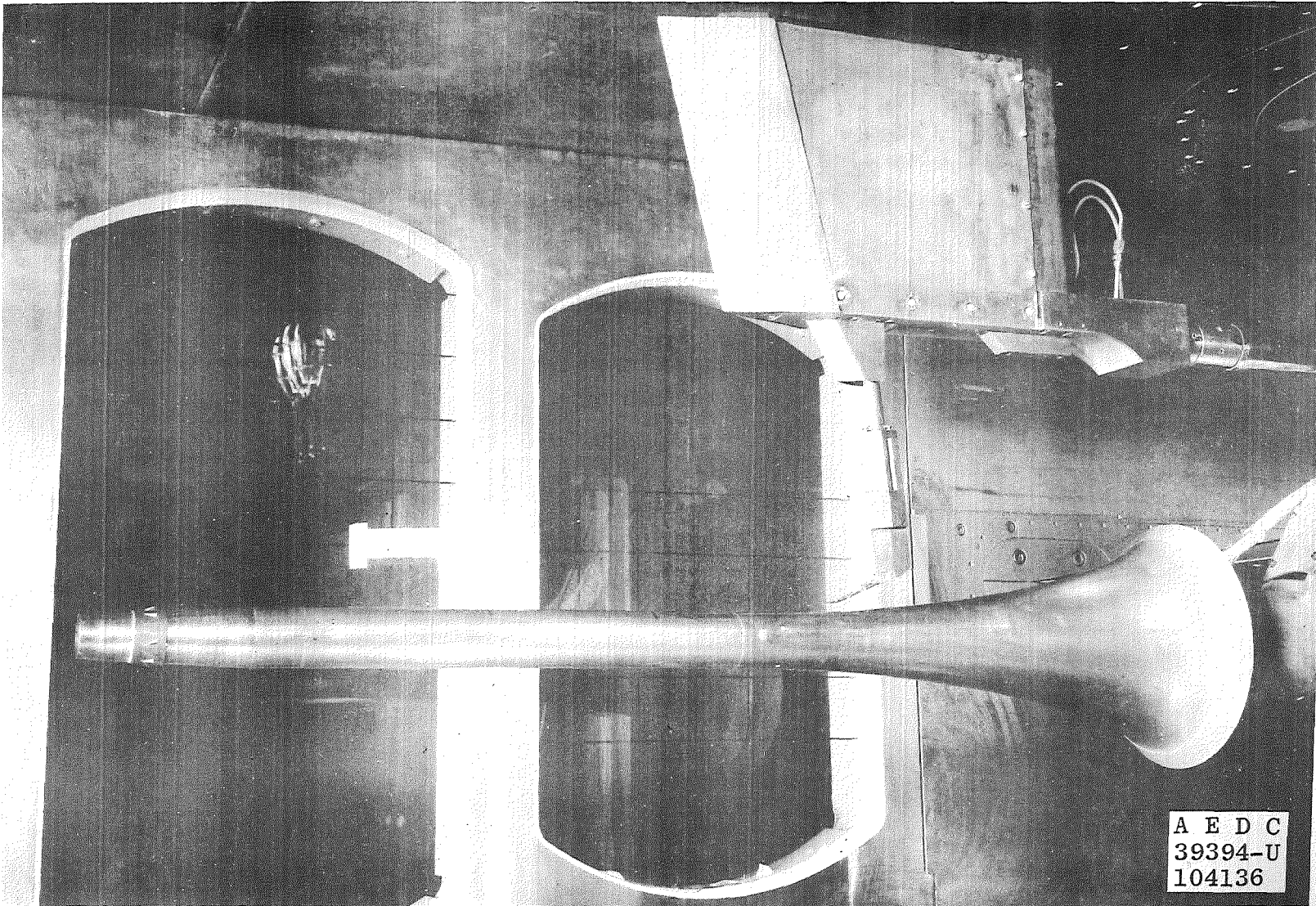
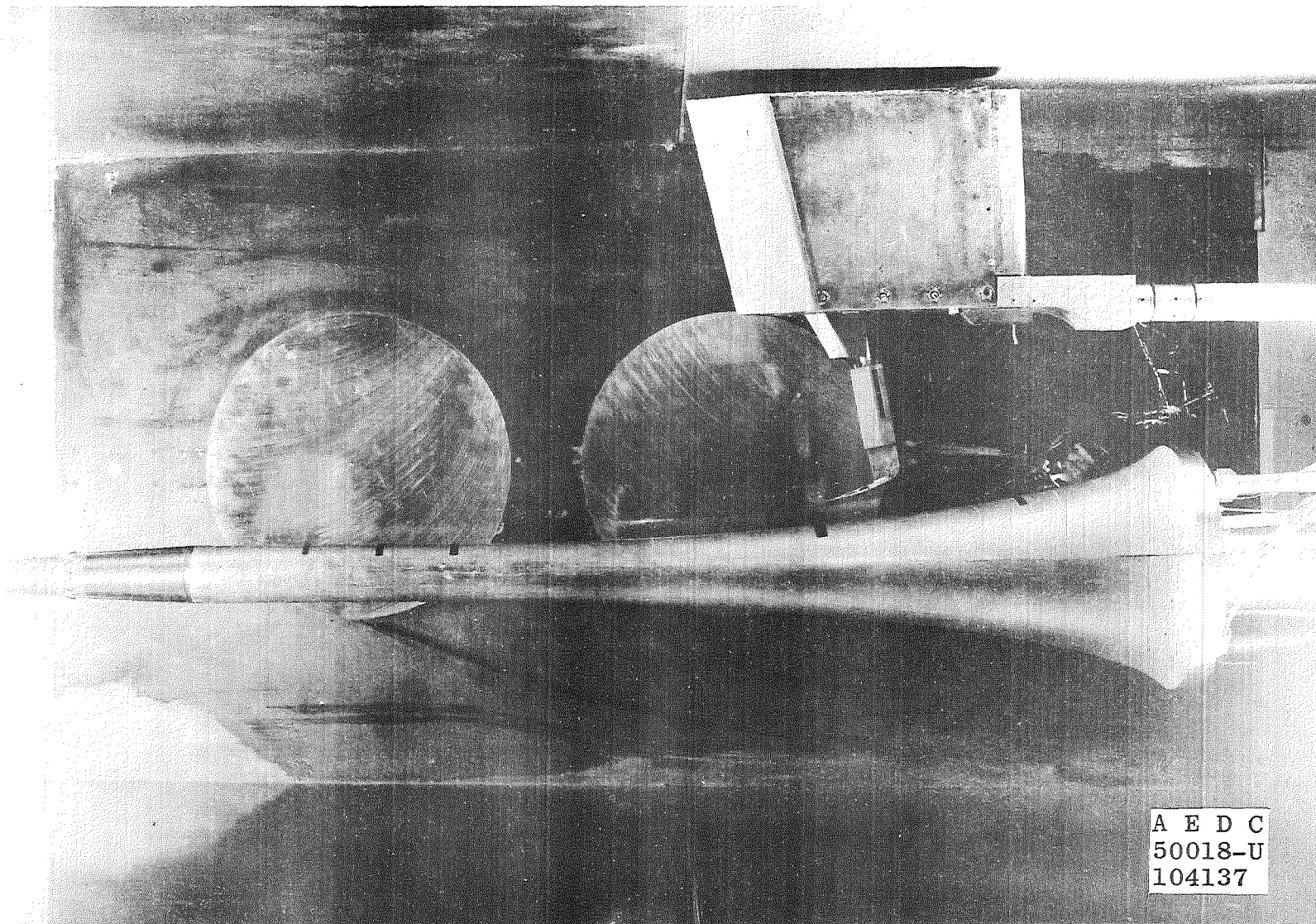


Fig- 6 Mach 8 Model Cooling Passages



a. C<sup>10</sup> G<sup>17</sup> TVGF

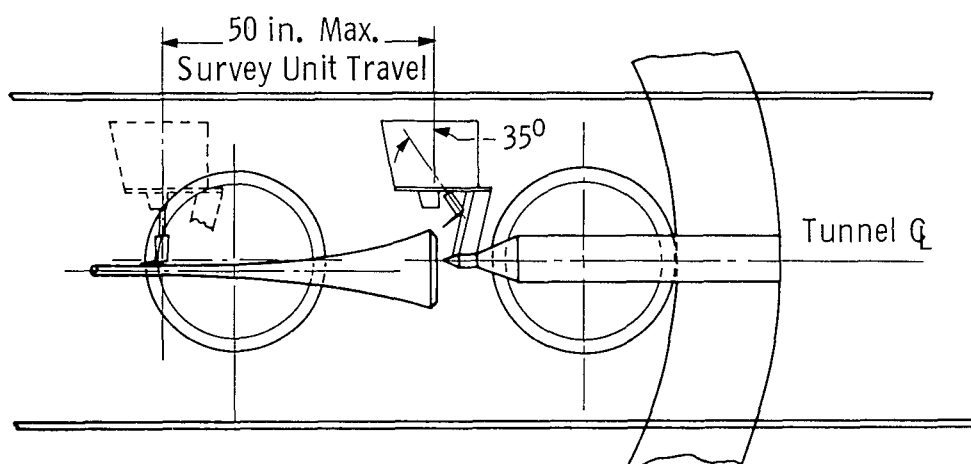
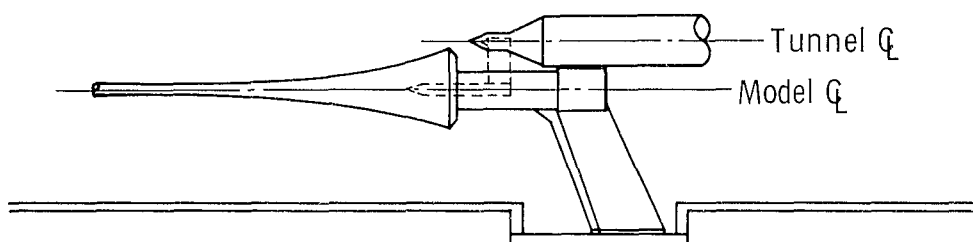
Fig. 7 Typical Model Installation in Tunnel A



A E D C  
50018-U  
104137

b. C<sup>8</sup>G<sup>12.5</sup> TVGF

Fig. 7 Concluded

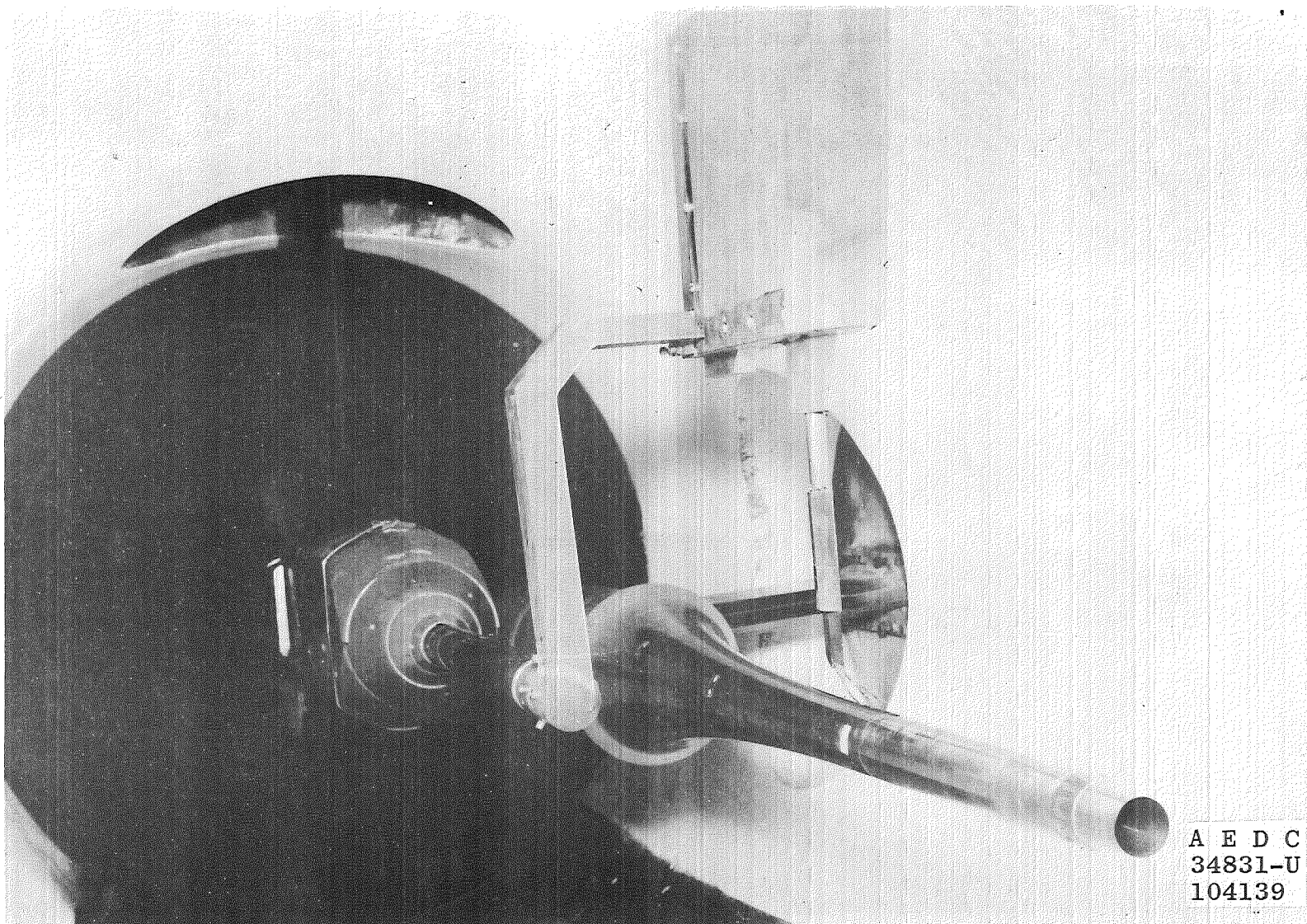


104138

a. General Sketch

Fig. 8 Typical Model Installation in Tunnel B

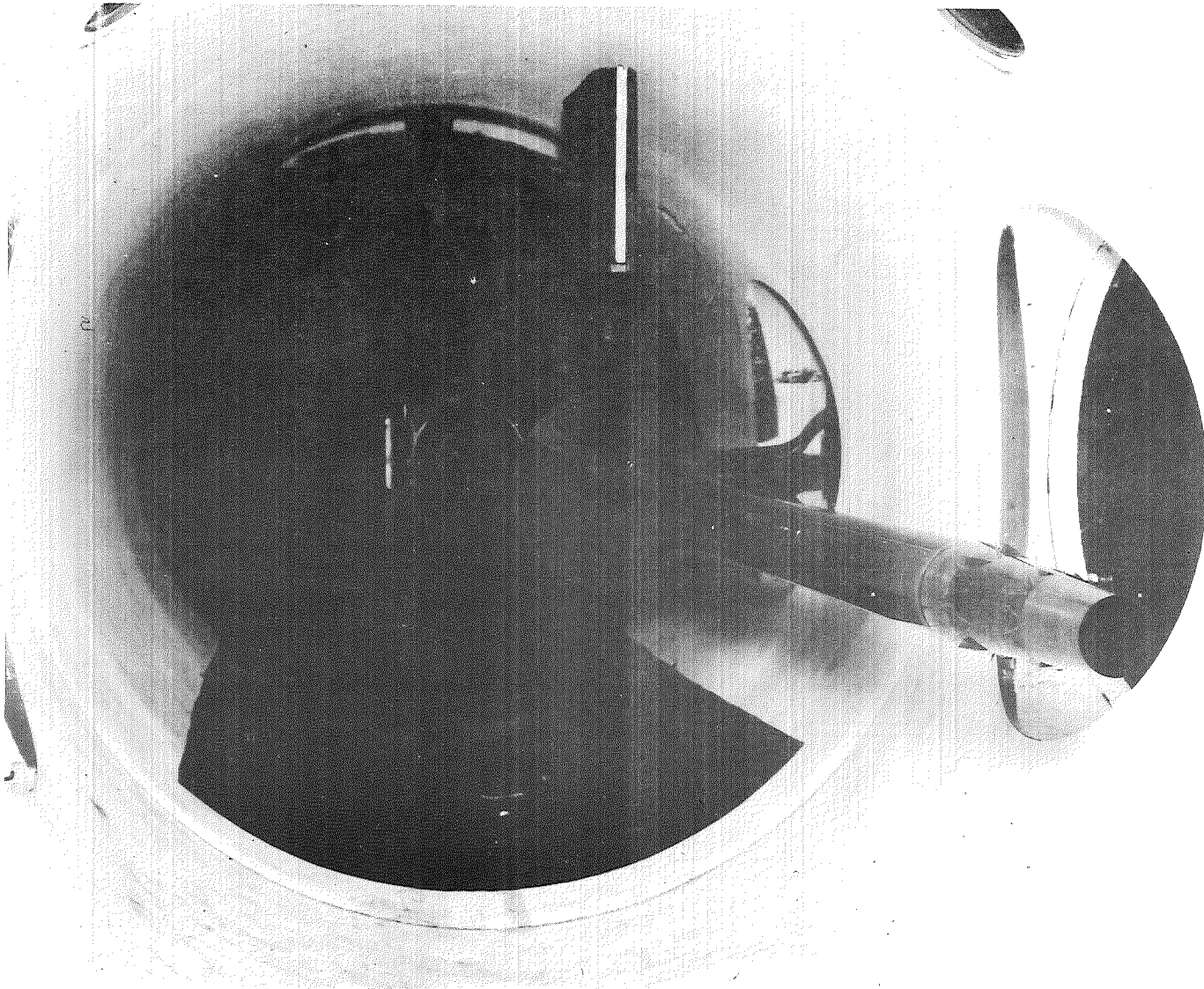




A E D C  
34831-U  
104139

b. C<sup>5</sup>G<sup>9</sup>TVGF

Fig. 8 Continued



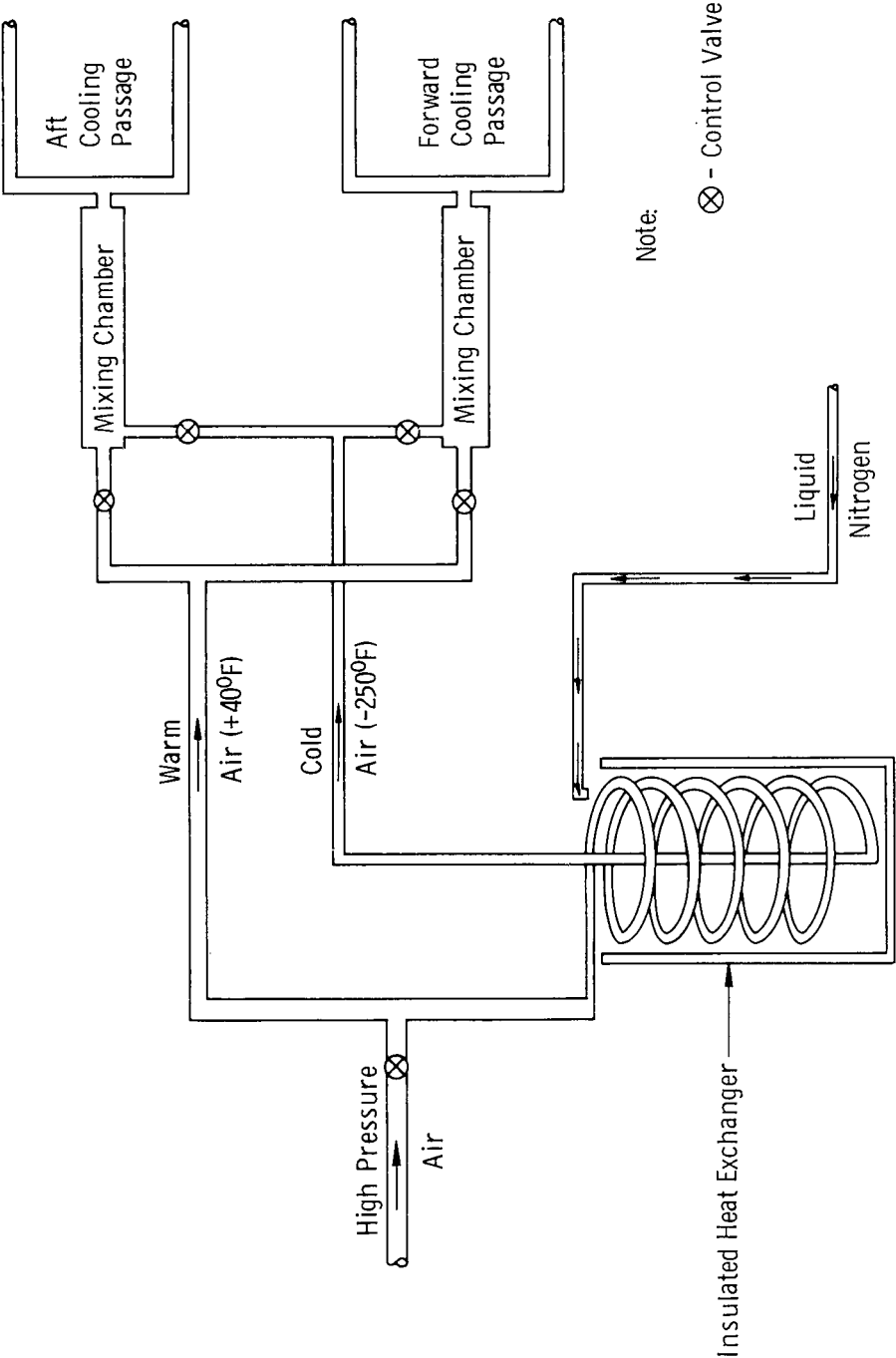
c. C<sup>8</sup> G<sup>12.4</sup> TVGF

Fig. 8 Concluded

A E D C  
47714-U  
104140

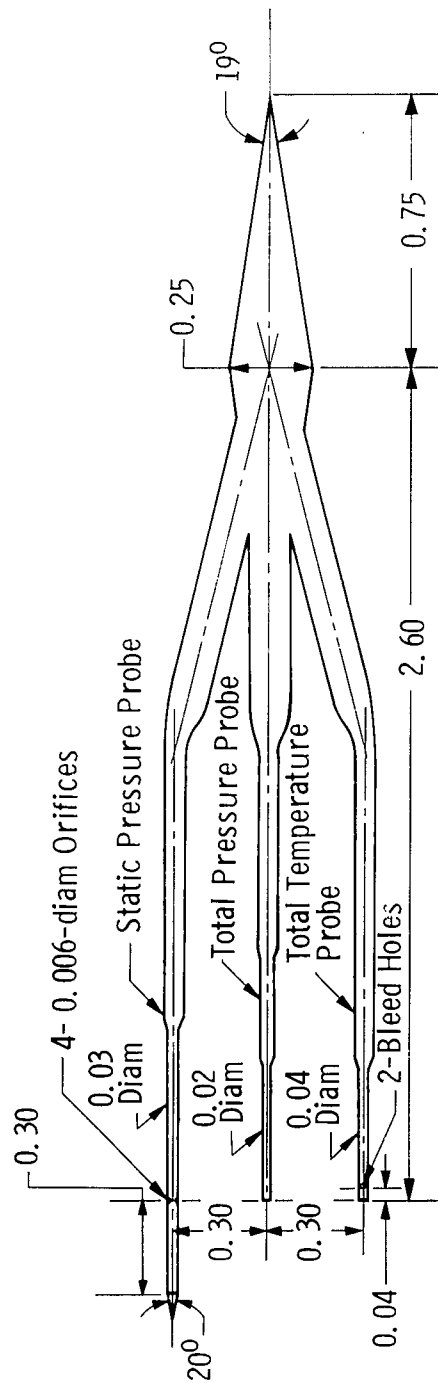
AEDC-TDR-64-268





104141

Fig. 9 Cooling System for Mach 8 Model



All Dimensions in Inches

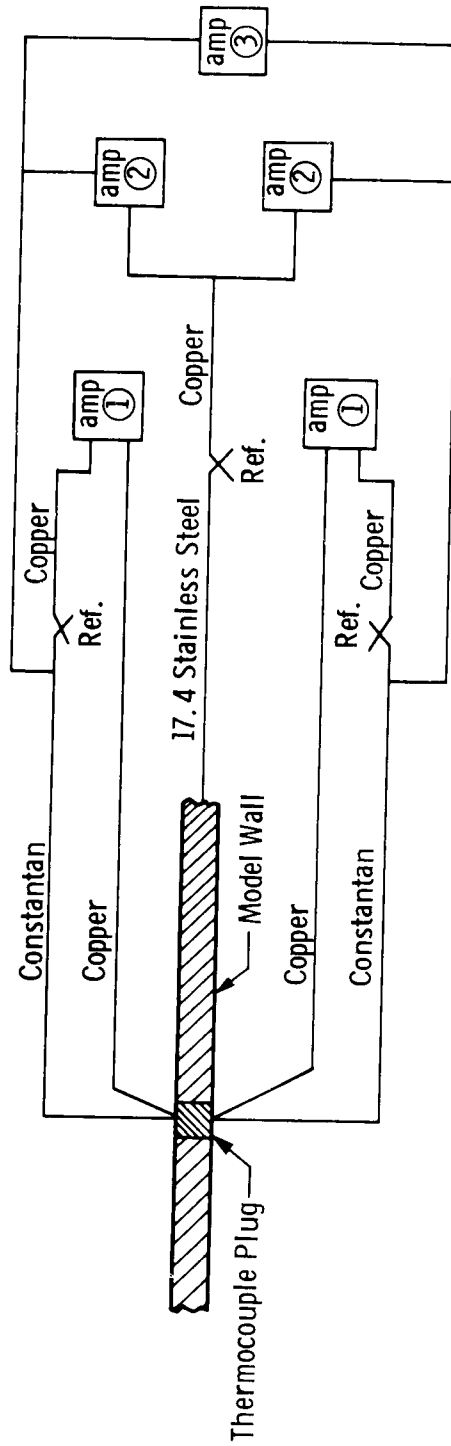
104142

Fig. 10 Geometry of the Triple Survey Probe



A E D C  
34836-U  
104143

Fig. 11 Triple Survey Probe Installed in Tunnel B



Notes: 1. All splices within the same circuit were maintained at the same temperature.

2.  - Standard Cu-Cn Thermocouple with 150°F Reference

3.  - Stainless Steel-Constantan Thermocouple with 150°F Reference

4.  - Differential Reading between Internal and External Temperatures

104144

Fig. 12 Typical Thermocouple Plug Wiring Diagram

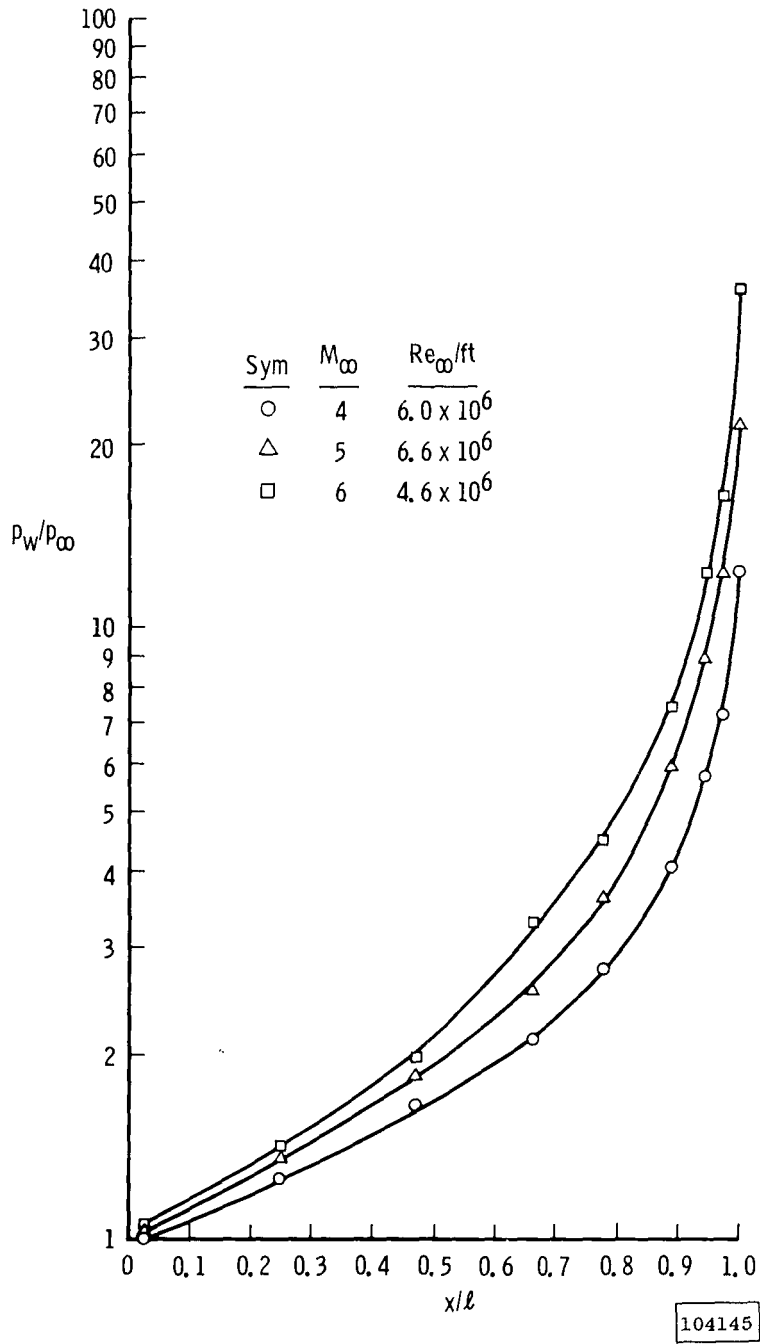
a. C<sup>5</sup>G<sup>17</sup>T<sup>VGF</sup>

Fig. 13 Compression Surface Pressure Distribution at Various Mach Numbers

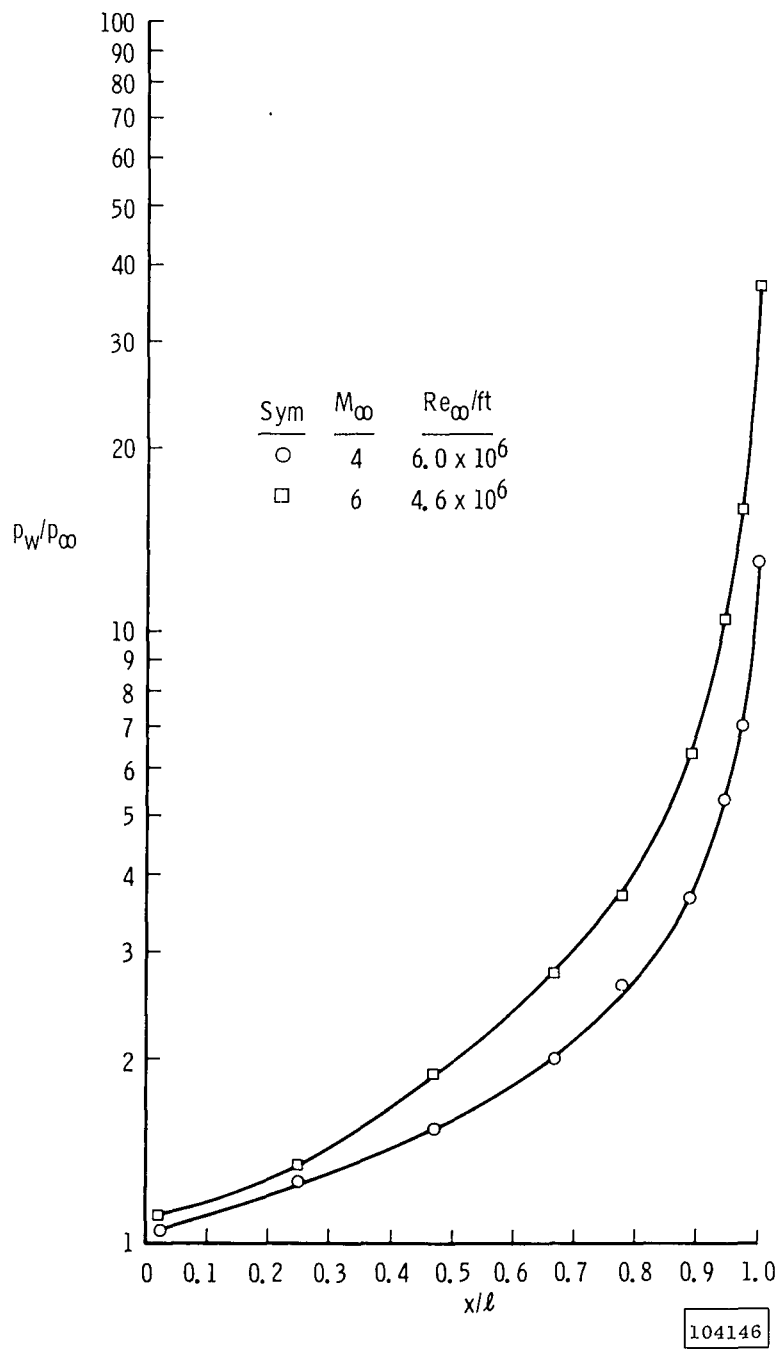
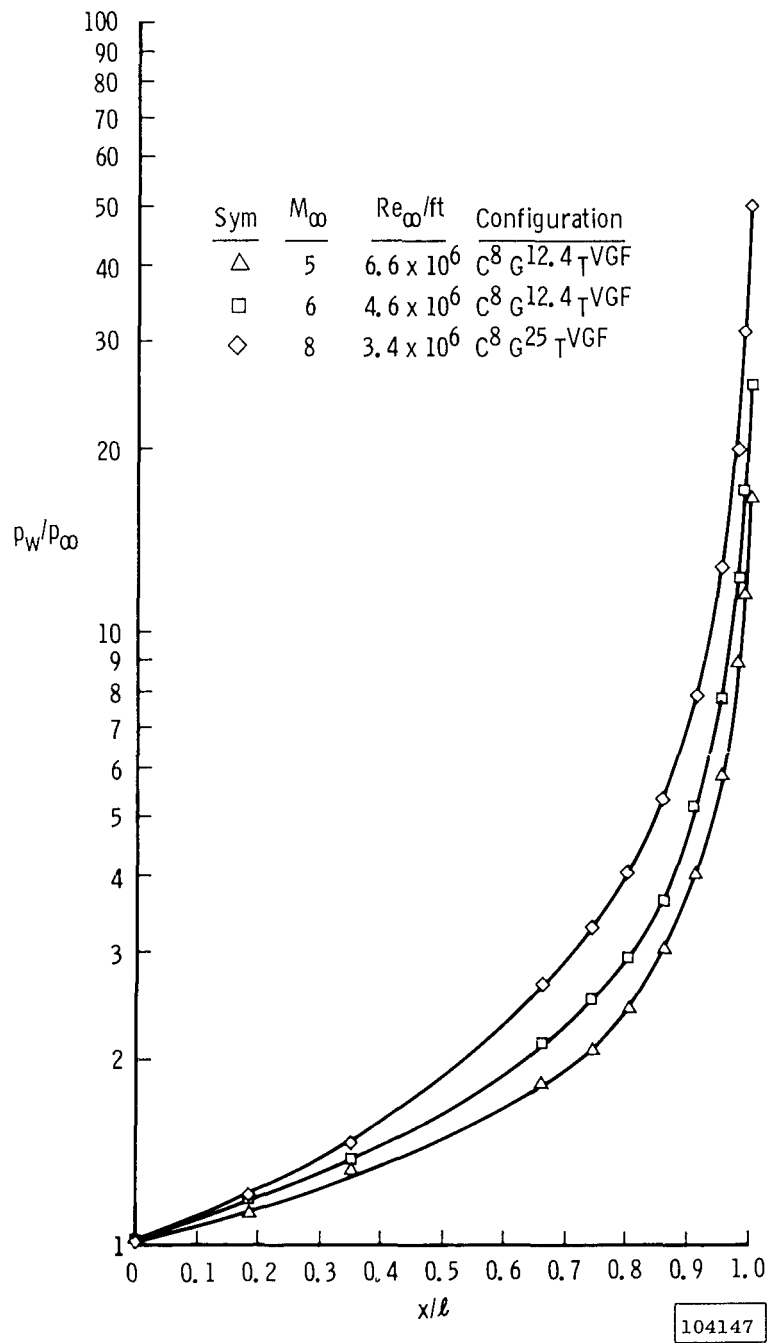
b. C<sup>6</sup>G<sup>17</sup> TVGF

Fig. 13 Continued



c. Mach 8 Model

Fig. 13 Continued

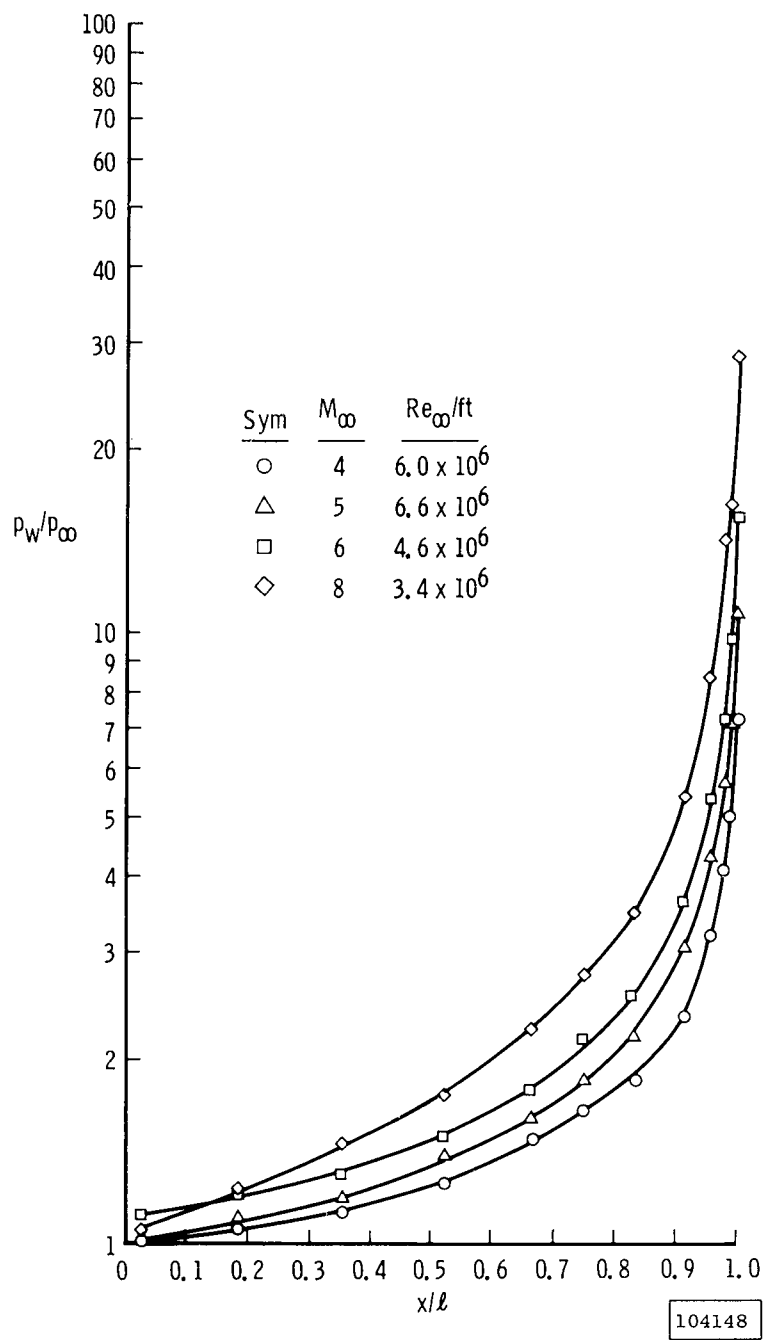
d. C<sup>10</sup> G<sup>17</sup> TVGF

Fig. 13 Concluded



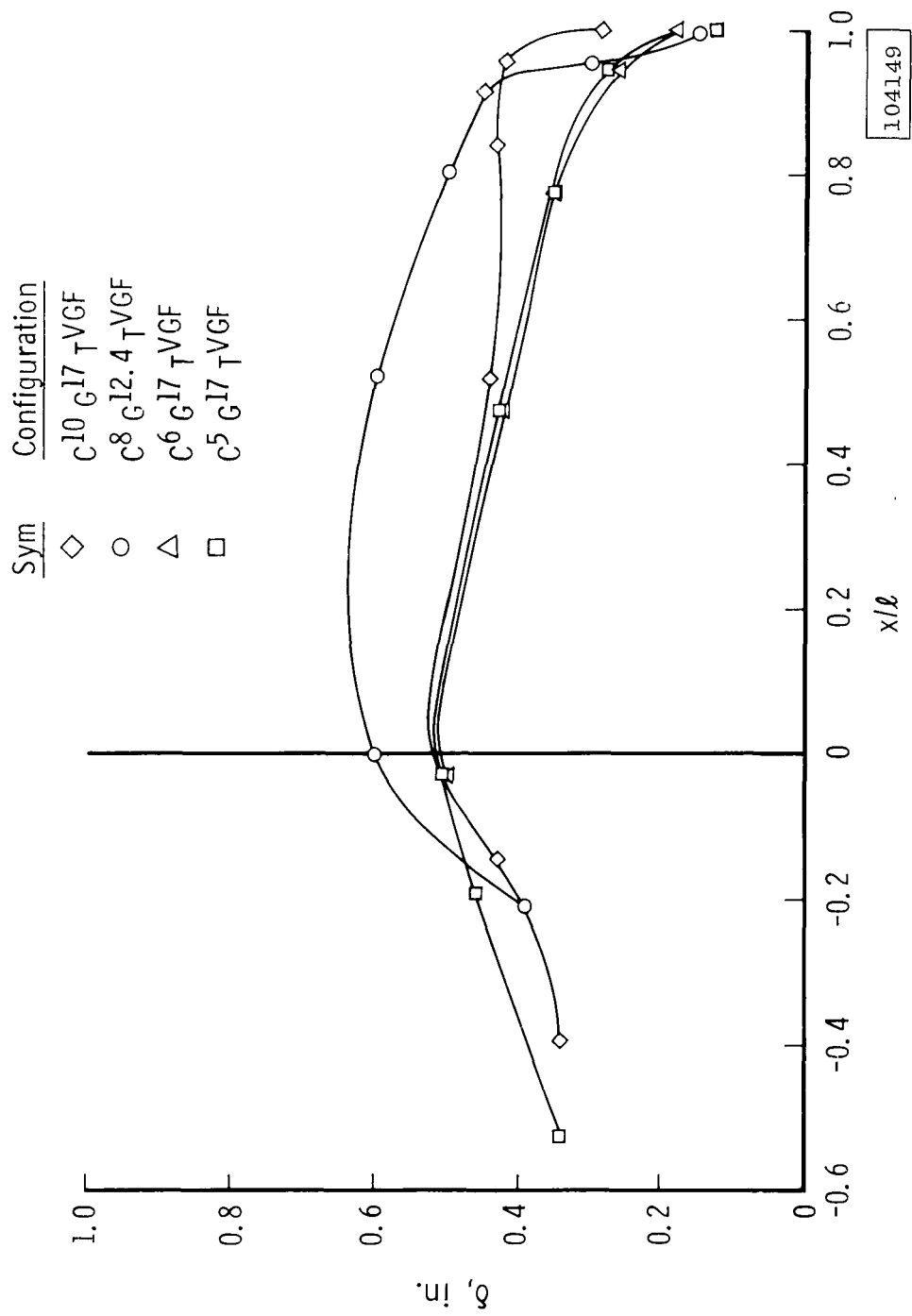


Fig. 14 Boundary-Layer Thickness for All Models at  $M_\infty = 6$ ,  $Re/ft = 4.6 \times 10^6$

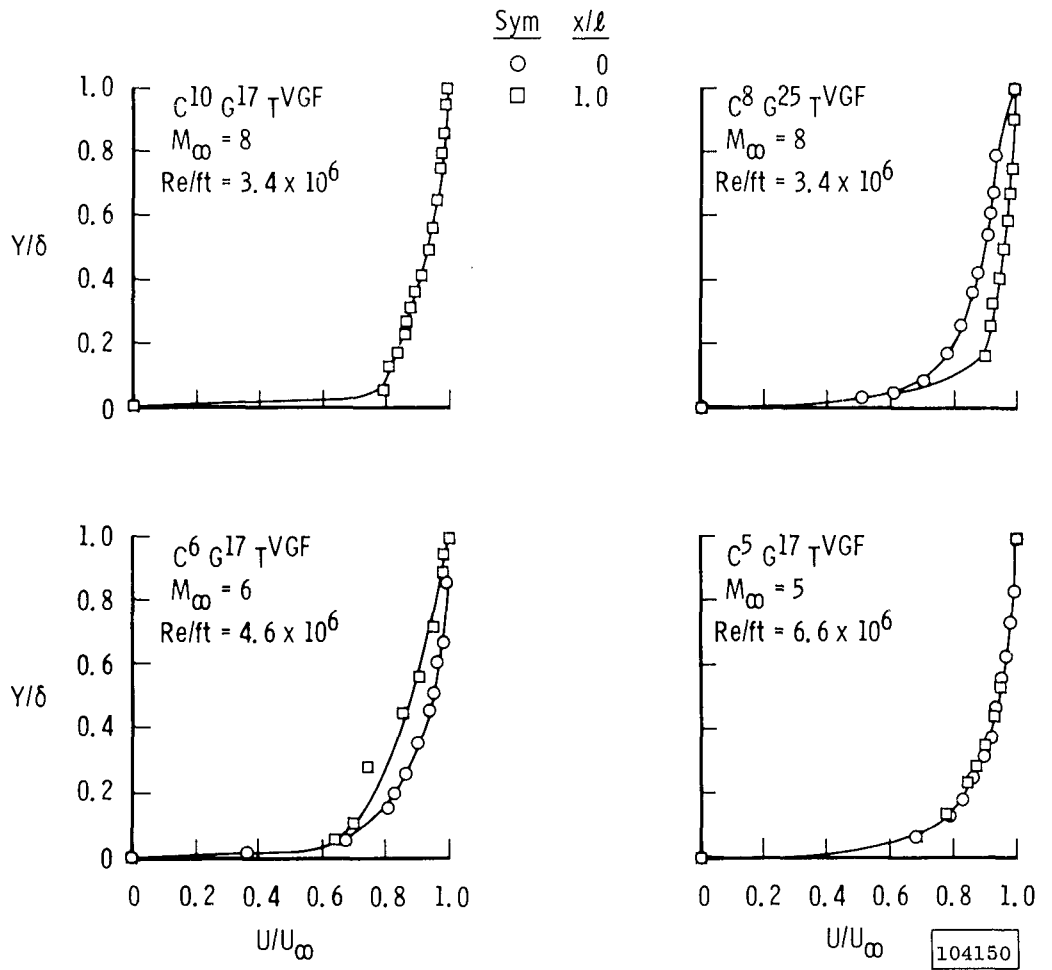


Fig. 15 Velocity Profiles for All Models at or near Design Mach Number

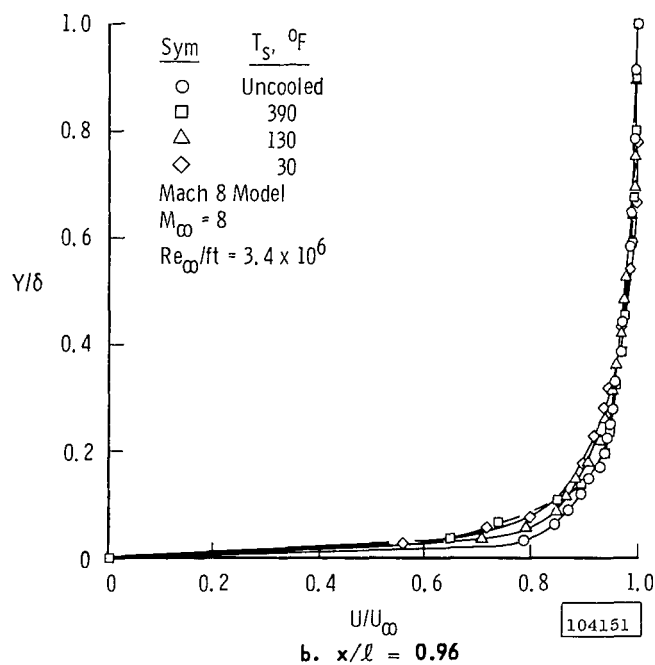
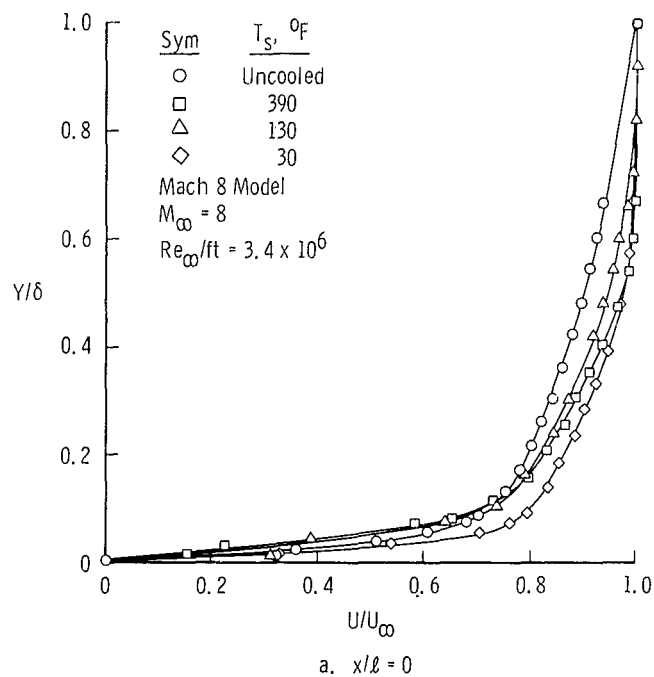


Fig. 16 Effect of Model Wall Temperature on Velocity Profile

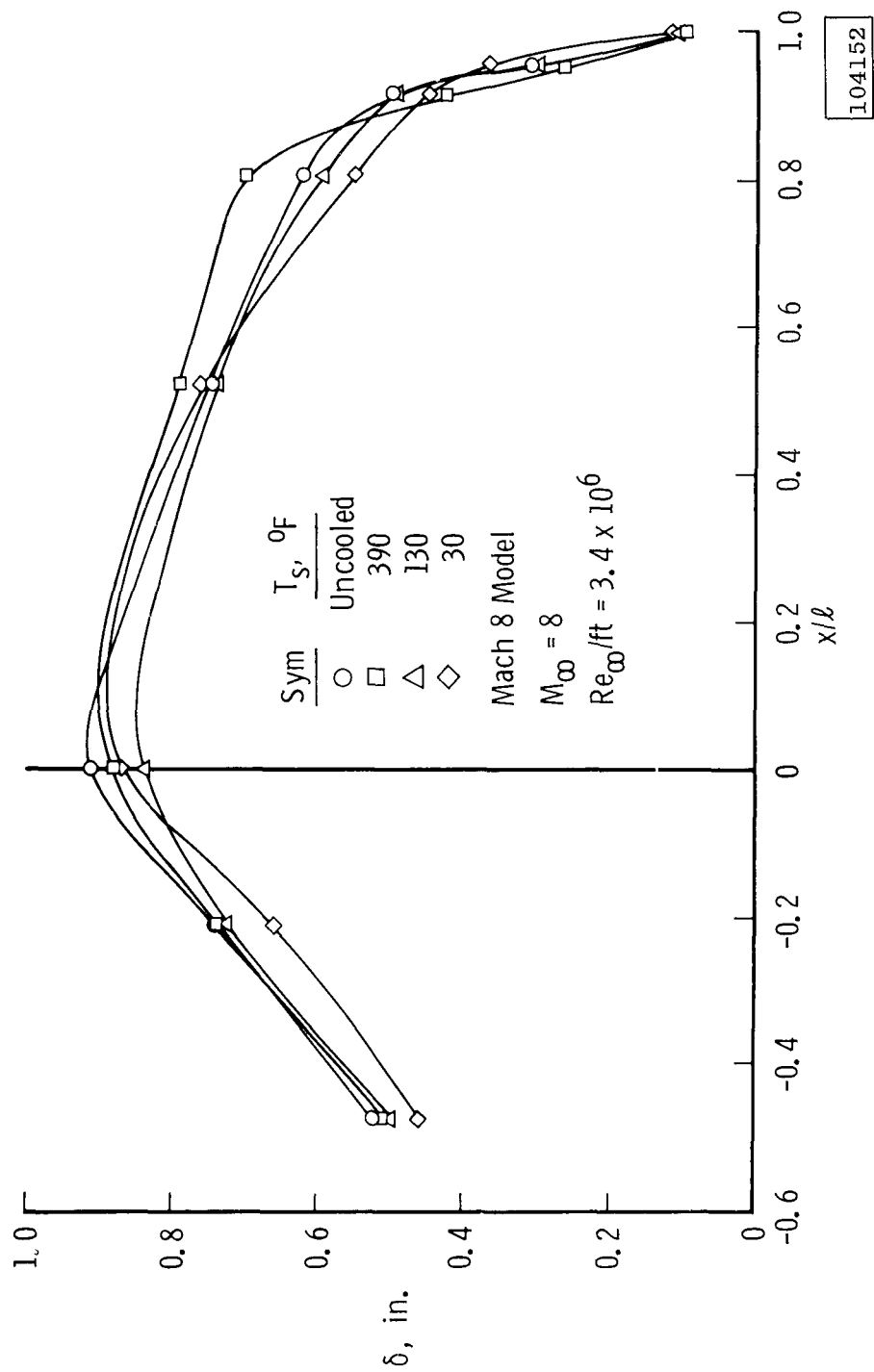


Fig. 17 Effect of Model Wall Temperature on Boundary-Layer Thickness